International Journal of Thin Film Science and Technology

Volume 12
Issue 1 *Jan. 2023*

Article 3

2023

Characterization of Indium Doped Tin Disulphide Thin Films using Modified Spray Pyrolysis Technique

G. Anbazhagan
Department of Physics, H.H.The Rajah's College, Pudukkottai - 622 001,Tamilnadu, India,
daniepappu@gmail.com

L.Amalraj
Department of Physics, V.H.N.S.N.College, Virudhunagar - 626 001, Tamilnadu, India,
daniepappu@gmail.com

K. Vijayakumar
Department of Physics, H.H.The Rajah's College, Pudukkottai - 622 001,Tamilnadu, India,
daniepappu@gmail.com

International Journal of Thin Films Science and Technology

http://dx.doi.org/10.18576/ijtfst/120103

Characterization of Indium Doped Tin Disulphide Thin Films using Modified Spray Pyrolysis Technique

G. Anbazhagan[1], L. Amalraj[2] and K.Vijayakumar [1,*]

[1]Department of Physics, H.H.The Rajah's College, Pudukkottai - 622 001,Tamilnadu, India
[2]Department of Physics, V.H.N.S.N.College, Virudhunagar - 626 001, Tamilnadu, India

Received: 2 Aug 2022, Revised: 4 Sep. 2022, Accepted: 16 Oct. 2022.
Published online: 1 Jan. 2023.

Abstract: Precursor solutions of tin tetrachloride monohydrate (0.1 M), n-n dimethyl thiourea (0.05 M, 0.1 M and 0.2 M) were used to prepare Tin disulphide (SnS_2) thin films had been deposited onto glass substrates at different molar concentration at the substrate temperature 573 K using modified spray pyrolysis technique. At the molar concentration ratio 1:2, the physical properties were studied for undoped and Indium doped tin disulphide thin films. Using hot probe technique, the films are found to be n type electrical conduction. X ray diffraction analysis revealed single phase tin disulphide thin film with higher intensity and belongs to hexagonal structure and the polycrystalline nature of a preferential orientation along (002) plane. The crystallites sizes were determined using the Full Width at Half Maximum values of Bragg peaks. SEM micrographs had shown that morphologies of the films changed with Indium doping. The optical absorption and transmittance spectra have been recorded for as prepared films in the visible wavelength range in nanometer. From the analysis of the absorption region data, direct and direct forbidden optical transition nature was determined for the films in the above wavelength range. FTIR study had been carried out for the bond evaluation.

Keywords: Hexagonal; Transmittance; Bragg peak; Band gap; Monophase.

1 Introduction

Metal chalcogenides were synthesized and characterized in thin film form prepared via different techniques have attracted extensive attention for the last few decades due to their potential applications in different fields. Tin chalcogenides belonging to the IV–VI group semiconductors are found to be superior candidates for optoelectronic and solar cell applications [1]. Different forms and their respective properties of several binary sulfides of tin were studied. Due to their electrical and optical properties, these binary compounds have a high potential use in optoelectronic devices and photoconductive cells [2, 3]. Tin sulphide is forming a multiplicity of phases such as SnS, SnS_2, Sn_2S_3, Sn_3S_4, etc. due to their varying coordinating characteristics of tin and sulfur. Amongst these semiconductors, tin disulphide (SnS_2) has CdI_2-type structure. Thin film of tin disulfide is composed of sheets of tin atoms sandwiched among two close-packed sheets of sulfur atoms [4] and has several properties like high optical absorption co-efficient (>10^4 cm^{-1}) in the visible region [5], n-type electrical conductivity [6, 7], wide optical band gap [8], etc. These properties support the use of this material as a window layer in thin film solar cells [9]. Ozin and co-workers [10] reported that excellent gas sensors can be fabricated for sensing NH_3, H_2S, or alcohols with nanoporous SnS_2.Thin films of SnS_2 were fabricated by various techniques like close-spaced sublimation [11], sulphurization of metallic precursors [12], atmospheric pressure chemical vapor deposition [13], chemical vapor transport [14], chemical deposition [15],vacuum evaporation [16,17], dip coating [18,19], solvo thermal process [20], chemical spray pyrolysis [21,22] and each method has its own characteristic advantages and drawbacks in producing homogeneous and defect-free thin film. Among them nebulized spray pyrolysis method is principal to prepare tin disulphide thin film, which is a low cost method that can be used to coat uniform deposition on large surface area [23] with less solution wastage. Since this new nebulized spray pyrolysis is method is capable of producing mist-like sprayed particles of the precursor solution, nano structured morphological surface with distinct semiconductor properties were probable. In this paper, it is intended to prepare and characterize undoped and Indium doped tin disulfide thin films on amorphous glass substrates using the precursor solutions of tin tetra chloride penta hydrate and thiourea by nebulized spray pyrolysis technique.

*Corresponding author E-mail: daniepappu@gmail.com

2 Experimental Details

Tin disulfide thin films were deposited onto amorphous glass substrates with different precursor concentrations of tin species by modified spray pyrolysis technique using the nebulizer. The precursor solutions of tin tetra chloride penta hydrate ($SnCl_4.5H_2O$) and thiourea ($CS(NH_2)_2$) were prepared separately using a solvent containing de-ionized water and isopropyl alcohol in 3:1 ratio, respectively. Two drops of concentrated hydrochloric acid were added for complete dissolution. An equal volume of Tin tetra chloride penta hydrate and thiourea solutions were mixed together and sprayed onto the hot glass substrates with an area of 75 × 25 mm^2. The deposition parameters like the substrate temperature, carrier gas pressure, volume of the solution, and nozzle to substrate distance were fixed as 573 K, 0.7 Kg/cm^2, 5 ml, and 2 cm, respectively. After deposition of these films, it was allowed to cool to room temperature, cleaned with distilled water, dried, and then stored in a dessicator. The crystal structure of these films was examined by the X-ray diffraction (XRD) pattern recorded using XPERT PRO diffractometer using Cu Kα radiation (k = 1.5406 Å). The scanning angle 2θ was varied in the range of 10–60° in steps of 0.05°. The surface morphology of the as-deposited SnS_2 thin films was recorded with a magnification of about 20 k by Carlzeiss (EV018) scanning electron microscope with a working distance of around 10 mm and the chemical composition of the films was recorded with the same instrument. The absorption spectrum was recorded in the wavelength range 400–800 nm using Shimadzu-UV 1800 model double beam spectrophotometer.

3 Results and Discussion

Structural Characterization

The color of the thin film prepared with concentration ratio 1:0.5 and 1:1 were pale yellow with less adhesion to the substrate. Thin films prepared with concentration ratio 1:2 had good adherence and were golden yellow in color. These films looked shiny with multiple color due to internal multiple reflections and golden yellow in color due to transmitted light. This variation in the color may be due to light variation in the temperature of the substrate which may be evident and prominent at higher concentration.

Fig 1 (a) – 1 (c) showed the XRD profiles of the nebulized spray pyrolytic SnS_2 thin films with various precursor concentration ratios 1:0.5, 1:1 and 1:2. The XRD pattern of the film at 1:0.5, (Fig.1 (a)), is obtained and has no definite peaks which may be attributed the nucleation kinetic process may not be exists. So, the concentration ratio increased to equimolar, three mixed phases are appeared ie. SnS_2 is observed (hexagonal) at 2θ = 14.49° with phase (002), 26.33 (SnS) with phase (021), and 31.58 (SnS) with phase (040),is shown in the fig 1(b) [JCPDS file no. 39-0354]. Furthermore at the concentration ratio increased to 1:2, monophase Bragg peak is appeared at 14.24° (SnS_2) [24]. The preferential orientation growth of SnS_2 compound having hexagonal structure along (002) plane at the precursor concentration ratio 1:2 [(Fig 1(c)] diffracted with single prominent Bragg peak at 14.24°. The observed peak position 2θ is in good agreement with the reported values of Thangaraju et al.

The interplanar spacing corresponding to this peak is determined to be 5.85 Å, which is lower than the standard value 5.905 Å which cannot be attributed to any other phase of tin and sulphur. The value of lattice parameter is determined to be 11.60 **Å** due to this hexagonal structure. It is found that the unit cell of this structure in the present study is shrinked in c direction while comparing with the standard report of 11.80 Å (file no. 89-3198). The strain may be attributed to higher molarity ratio of this compound and this ratio affects the nucleation kinetics resulting in a change of critical nucleus size and the rate of nucleation [25]. Authors [26] had observed strain in their SnS_2 thin films prepared by SILAR and plasma enhanced chemical vapor deposition methods respectively. From the Full Width at Half Maximum (FWHM) value of the peak obtained, size of the tin disulphide crystallites was determined using Debye Scherrer formula [27]. Fig. 2 shows the X-ray diffraction spectra of the undoped and indium doped SnS_2 films at molar ratio 1:2. The films exhibit the hexagonal structure along (002) plane and the d-values are well consistent with the standard data (JCPDS 89–3198). The lattice parameters 'a' and 'c' are in good agreement with the standard data.

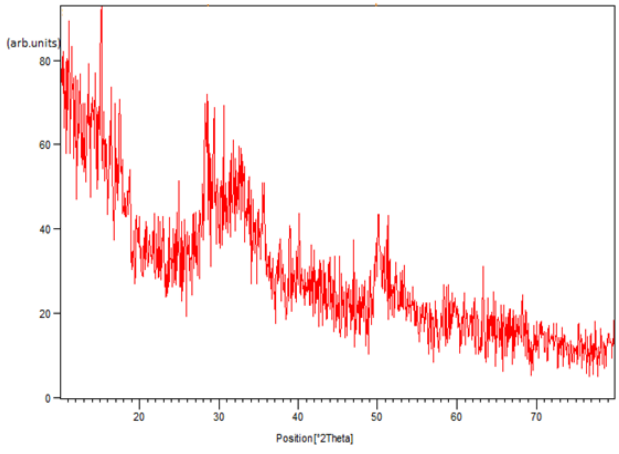

Fig. 1: (a) XRD patterns of SnS_2 thin film at ratio 1:0.5

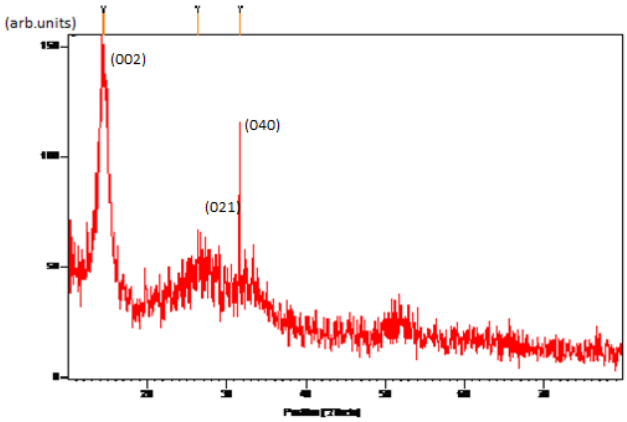

Fig.1 (b): XRD patterns of SnS_2 thin film at ratio 1:1.

The thickness of the films estimated from gravimetric method. The size of crystallite is estimated by the Scherrer's formula.

$$D = k\,\lambda / \beta \cos\theta$$

where K= 0.9 is the shape factor, λ is the X-ray wavelength of CuKα radiation, θ is the Bragg's angle and β is the full width half maximum of the peaks and is their lattice strain and the value of dislocation density (δ) is calculated and tabulated in table 1.

It is clear that the Crystallite size of SnS_2 is decreases when Indium doping, similar values of crystallite size of spray pyrolytic SnS_2 thin film is 60 nm [28] using same precursor solutions $SnCl_4$. $5H_2O$ and thiourea.

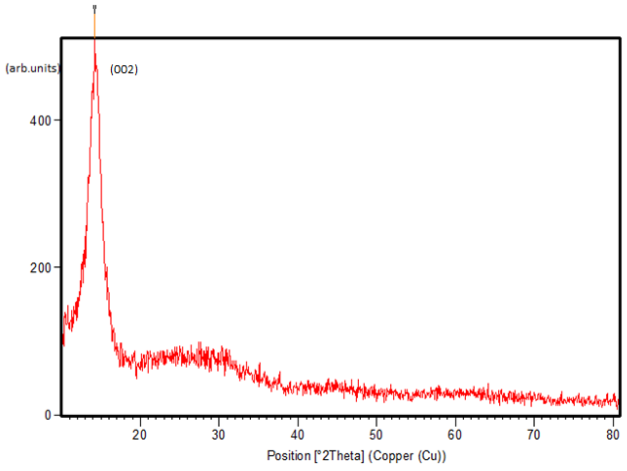

Fig.1 (c): XRD patterns of SnS_2 thin film at ratio 1:2.

The reflected intensity of the most intense peak of the SnS_2 film increases with the indium doping also found that above ratio 1:2. Author had [29] reported the similar result of indium doping SnS_2 thin film and is good agreement with the present data.

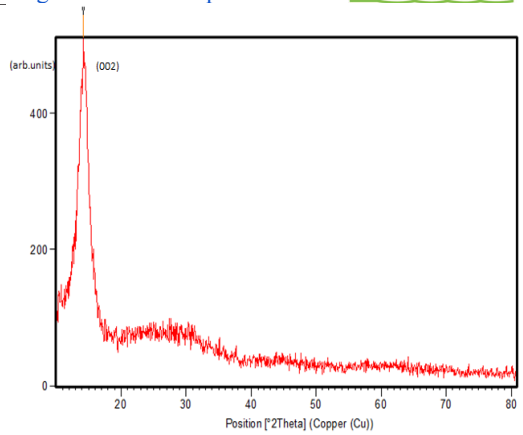

(a)

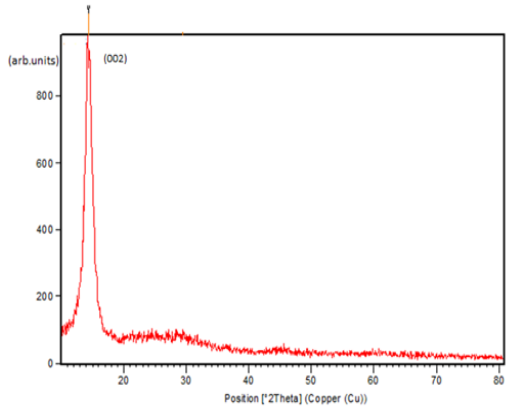

(b)

Fig.2: XRD patterns of (a) undoped (b) SnS2 :In (6 at %) thin film at 1:2 molar ratio.

The micro structural parameters like crystallite size, strain and dislocation density have been calculated and shown in table 1.The strain and dislocation density increases with crystallite size decreases with respect to the Indium doped tin disulphide thin film.

The SEM with a magnification of 20 k of the undoped and In-doped SnS_2 thin films at 573 K and molarity ratio 1:2, are shown in figure 3 (a) and (b) respectively. The formation of spherical shape grains with a layer by layer texture for undoped and In-doped thin film respectively. SEM images show the grain size ranges from 35.5–39.5 nm and 48.7–56.9 nm and nm for undoped and doped films respectively. It is observed that the films doped with Indium exhibit a change in the surface morphology, increased grain size and homogeneous distribution of grains. The grain size is measured by the average distance between the visible grain boundaries. Each grain constitutes aggregates of several crystallites [30].

Table 1: Structural parameters of undoped and Indium doped thin films.

Precursor concentration ratio (1:2)	2 theta value (degree)	d spacing values (A°)		lattice constant (A°)		Crystallite size (nm)	Strain x 10^{-3} lines $^{-2}$ m^{-4}	Dislocation density x 10^{14} nm^{-2}	No.of crystallites x 10^{17}	Thickness (nm)
		observed	JCPDS	observed	JCPDS					
Undoped SnS_2	14.38	6.15	5.90	3.63	3.64	97.16	3.567	105.93	6.25	574
In-doped SnS_2	14.24	6.21	5.92	3.68	3.60	59.14	5.860	285.91	23.25	481

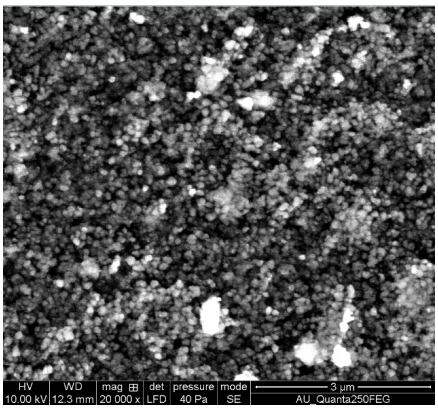

(a)

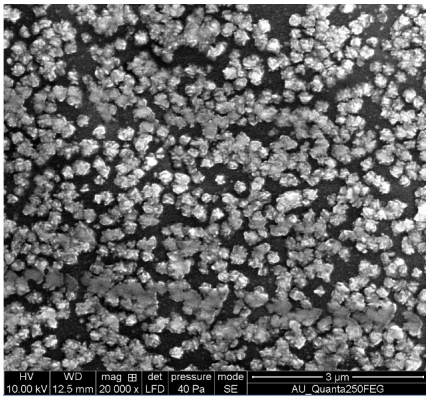

(b)

Fig. 3: SEM images of (a) undoping SnS_2 (b) SnS_2 : In (6 at%) thin films.

The films had a thickness is measured by gravimetric method. The optical transmittance of the films measured in the wavelength range 400-800 nm was used to calculate the absorption coefficient α. The dependence of absorption coefficient on photon energy is of important in studying energy band structure and the type of transition of electrons.

The optical transmittance (T) of the film is measured in the wavelength range 400–800 nm at room temperature for undoped and doped films as shown in figure 5. The spectra indicate a smooth increase and almost saturate at 75 % transmittance for both undoped and In-doped thin films. This smooth increase is due to high crystalline nature of the prepared film. The transmittance value of the doped films is found to be less than undoped film over the entire range of wavelength. Author Thangaraju et al. had reported the similar results at the substrate temperature 573 K.

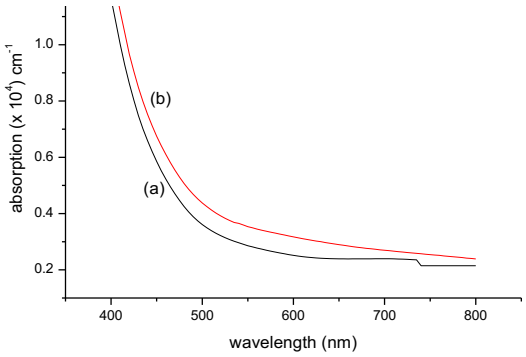

Fig.4: Absorption spectrum of (a) undoping (b) Doping SnS2 : In (6 at%) thin films

The relation between the absorption coefficient (α) and the incident photon energy hυ is given by

$$(\alpha h\upsilon)^2 = A\,(h\upsilon - E_g) \text{ ----------} \quad (1)$$

Where A is a constant and E_g is the band gap energy.

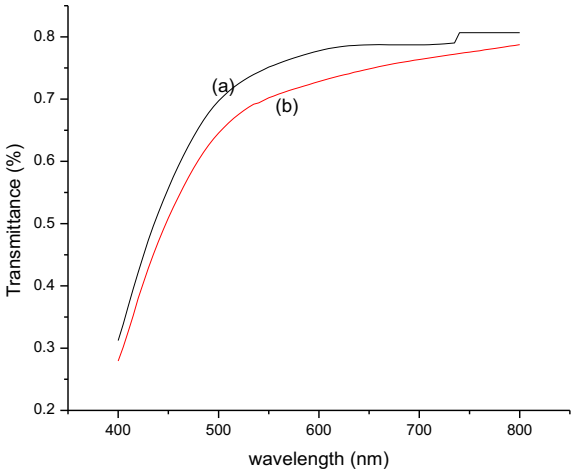

Fig 5: Transmittance spectra of (a) undoping (b) Doping SnS_2:In (6 at %) thin films at 1:2

To study the optical properties of the materials, the optical absorption spectra of the film is recorded in wavelength range 400 nm – 800 nm from which the absorption coefficient is calculated and plotted (Fig 4). It varies from the value of 1.3 x 10^4 cm^{-1} to 0.3 x10^4 cm^{-1} for doped thin film which is little higher than undoped thin film. The optical absorption spectra of tin disulphide thin film have been investigated for the evidence of either allowed or forbidden direct transition in accordance with the theory of Bardeen et al [31].

An analysis of eqn.1 which relates the absorption coefficient α, with the band gap Eg as provides the information about the type of optical transition takes place in semiconductor thin films. Both $(\alpha h\nu)^2$ versus photon energy hν have been plotted in fig 6 (a). The plot yields a straight line which indicates a good fit, extrapolation of the straight line to $(\alpha h\nu)^2$ gives the optical band gap values for undoped and Indium doped thin film. The band gap energy decreases from 2.76 eV for undoped SnS_2 film to 2.68 eV, in the case of direct forbidden optical band gap energy values decreases from 2.2 eV for undoped SnS_2 film to 2.05 eV [fig 6 (b)] for SnS_2: In thin film doped with indium concentration 6%. This decreased band gap values good agreement with the reported values by Thangaraju et al.

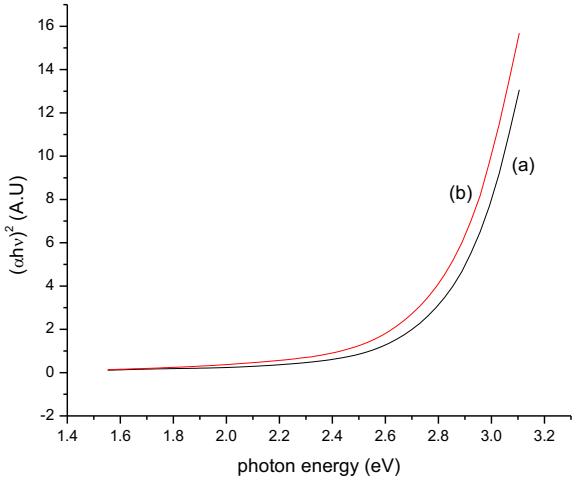

Fig.6 (a): $(\alpha h\upsilon)^2$ vshν of (a) undoping (b) Doping SnS_2:In (6 at %) thin films at ratio 1:2

When using the hot probe technique for the film under present study the current flow was from the cold junction to the hot junction. Hence the thin films prepared by spray pyrolysis in the present study were an n-type semiconductor. This ensures that the majority carrier of current is electrons. The Fourier transform infrared spectrum of the undpoed SnS_2 thin film at molar concentration 1:2 was shown in Fig 7 (a). The presence of bonding between Sn and S atoms is estimated from the FTIR spectrum recorded using the as prepared samples.

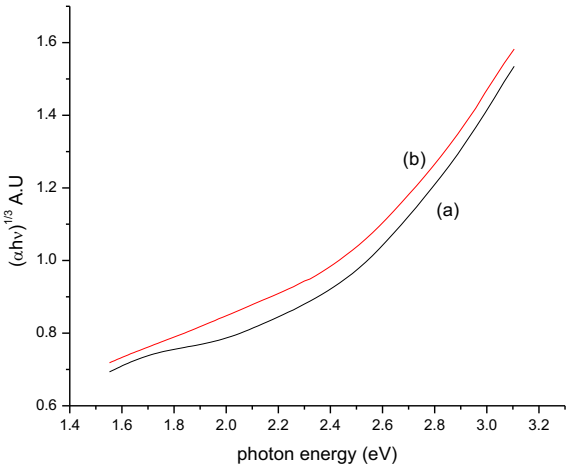

Fig.6 (b): $(\alpha h\upsilon)^{1/3}$ vshν of (a) undoping (b) Doping SnS_2:In (6 at %) thin films at ratio 1:2

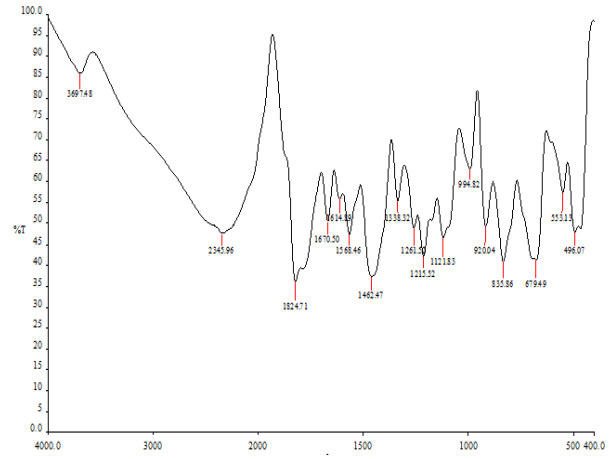

Fig.7(a): FTIR spectrum of undoped SnS_2 thin film at molarity ratio 1:2.

It indicates a broad band at 3697 cm^{-1} which corresponds to the vibration mode of O–H group indicating the presence of smallamount of water absorbed on the surface. The presence of strong C–H stretching at 2345 cm^{-1} is probably due to atmospheric moisture and CO_2 respectively, in the SnS_2 lattice. The formation of vibration band at 1824 cm^{-1} attribute to the hydroxyl group, it is good agreement with [32].

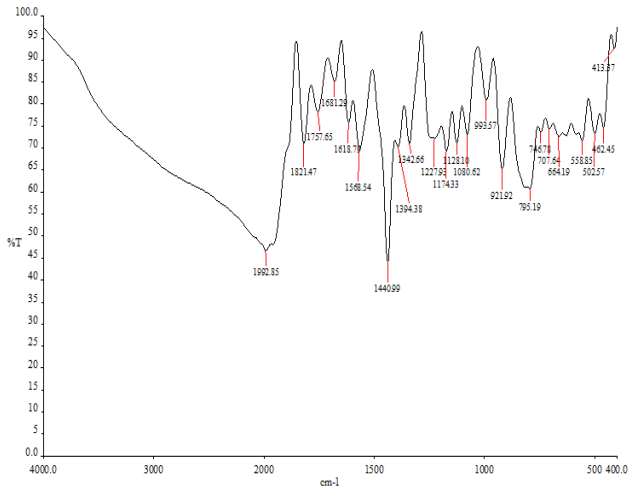

Fig.7 (b): FTIR spectrum of In-doped SnS_2 thin film at molarity ratio 1.

Indium doping FTIR spectrum of the SnS_2 thin film indicate a broad band at 1992 cm^{-1} which corresponds to the vibration mode of O–H group indicating the presence of small amount of water absorbed on the surface. The presence of strong C–H stretching at 1821 cm^{-1} is probably due to atmospheric moisture and CO_2 respectively, in the SnS_2 lattice [Fig 7 (b)]. The formation of vibration band at 1757 cm−1 attribute to the hydroxyl group.

4 Conclusions

Undoped and Indium doped SnS_2 thin films have been prepared by modified spray pyrolysis technique at the substrate temperature 573 K and molar concentration ratio 1:2. The XRD studies have shown that films formed at the ratio 1:2 is well oriented along the (002) plane. The crystallite size of Indium doped thin film was decreased when compared with undoped films. The most significant changes in structure are observed while doping in SEM micrograph. The analysis of optical transmission spectra reveals the existence of direct transition. The energy band gap value of the doped films is less than the undoped films. From our experiments, the physical properties of SnS_2 thin film can be modified by indium doping. From the structural and optical properties of tin disulphide thin films, which exhibit the potential candidate for opto electronic as well as thin film solar cell devices.

References

[1] H.Noguchi, A. Setiyadi , H. Tanamura, *Sol. Energy Mater. Sol. Cells.,***35**, 325, (1994).

[2] B.Thangaraju , P. Kaliannan , *J. Phys. D: Appl. Phys*.,**33** , 1054, (2000).

[3] L.Amalraj , C. Sanjeeviraja , M. Jayachandran , *J.Cryst. Growth.,***234** , 683, (2002).

[4] D.L.Greenaway , R.Nitsche , *Phys Chem Solids.,* **26**, 1445–1458, (1965).

[5] B.Thangaraju , P.Kaliannan , *J .Mater .elec,* **33**, 1059, (2010).

[6] A.Alam , S.Kumar , D.K.Singh *Materials today ,* **62,** 6102 **,** (2022).

[7] N.G.Deshpande, A.A.Sagade, Y .G. Gudage, *J Alloys Compd.,* **436**, 421–426, (2007).

[8] B.R.Sankapal, R.S. Mane, C.D.Lokhande , *Mater Res Bull.,* **35**, 2027–2203, (2000).

[9] C.Shi , Z.Chen , G.Shi , *Thin Solid Films.,* **520**, 4898– 4901, (2012).

[10] G.A.Ozin , T.Jiang , A.Verma , *J Mater Chem.,* **8**, 1649–1656, (2016).

[11] C.Shi , P.Yang, M.Yao, *Thin Solid Films.*, **534**, 28–31, (2013).

[12] J. Malaquias , P.A.Fernandes, *Thin Solid Films.,* **519**, 7416–7420, (2011).

[13] L.S.Price , I.P.Parkin, Hardy , *Chem Mater.,* **11**, 1792–1799, (1999).

[14] K.Matsumoto, K.Takagi , *J Cryst Growth.,* **63**, 202–204, (1983).

[15] C.D.Lokhande , *J Phys D Appl Phys.,* **23**, 1703–1705, (1990).

[16] K.Kawano , R.Nakata , M.Sumita, *J Phys D Appl Phys.,* **22**, 136–141, (1989).

[17] J.George , K.S.Joseph , *J Phys D Appl Phys.,***15**, 1109–1116, (1982).

[18] S.K.Panda, A.Antonakos, E.Liarokapis, *Mater Res Bull.,* **42**, 576–583, (2007).

[19] C.Sekar Ray, M.K.Karanjai ,D.Das Gupta, *Thin Solid Films,* **350**, 72–78 , (1999).

[20] B.Hai, K.Tang , C.Wang , *J Cryst Growth ,* **25**:92–95, (2001).

[21] C.Khelia , K.Boubaker , T.B.Nasrallah, *J Alloys Compd.*, **477**, 461–467, (2009).

[22] K.Vijayakumar , C.Sanjeeviraja , L.Amalraj,. *J Mater Sci: electron.,* **22**, 929–935, (2011).

[23] N.K.Reddy , K.T.R.Reddy , *Mater Chem Phys.,***102**, 13–18, (2007).

[24] X Ray diffraction JCPDS file no. 89-3198.

[25] B.Hai , K. Tang, C. Wang, *J. Cryst. Growth.,***225**, 92 ,(2001).

[26] B.G.Jeyaprakash, R. Ashok kumar, A. Amalarani, *J. Am. Sci.* **6**, 22 , (2010).

[27] B.Thangaraju, P.Kaliannan,*Cryst.Res.Technol.,***35**, 71(2000).

[28] K.Deva Arun Kumar , S. Valanarasu, L. Amalraj,*J.Mat.elec.,* 10854-017-7278, (2017).

[29] K.Santhosh Kumar, C.Manoharan, *Crystal Res.Tech.*,**47**, 771-779, (2012).

[30] R.N.Panda, M.F. Hsieh, R.J. Chung, *J. Phys. Chem. Solids .,* **64**, 193–199, (2003).

[31] J.Bardeen, F.J. Blatt, L.H. Hall, in *Proceedings of the Photoconductivity Conference, Atlantic city* (Wiley, New York,) p. 146. (1956).

[32] R.Mariappan, M. Ragavendar, V.Ponnuswamy, *Opt. Appl.phy.,* **4**, 989–997, (2011).